Are Ballasted Roof Systems Cool?

André Desjarlais
Thomas Petrie, PhD
and William Miller, PhD
Oak Ridge National Laboratory
Oak Ridge, Tennessee

ABSTRACT

It is well known that the mass of a ballasted roof can reduce peak roof temperatures and delay the heat flow into a building. However, ballasted roofs do not meet the requirements set out by the Environmental Protection Agency (EPA) and other organizations regarding being "cool roofs." To address whether ballasted roofing systems offer similar energy efficiency benefits as cool roofs, a project to perform side-by-side experiments was initiated. Three different weightings of ballasted roofs were installed next to a paver system and black and white membranes. Data collection included continuous monitoring of temperatures, heat flows, and weather conditions as well as periodic verification of the surface properties (solar reflectance and infrared emittance). These data are needed to determine what impact a ballasted roof has on heat flow into a building and on roof surface temperature. Furthermore, comparisons between the ballasted and unballasted membranes will allow for an assessment of whether ballasted systems perform as well as white membranes.

SPEAKER

André Desjarlais is the group leader for the Building Envelope and Materials Research Programs at the Oak Ridge National Laboratory. He has been involved in building envelope and materials research for over 35 years, first as a consultant and, for the last 16 years, at ORNL. He is active in the building industry, participating in ASHRAE, ASTM, Cool Roof Rating Council, SPRI, ARMA, Roof Industry Committee on Weather Issues (RICOWI), Federal Roofing Committee, and the Building Environment and Thermal Envelope Council. Areas of expertise include building envelope and material energy efficiency, moisture control, and durability.

Contact Information: Phone – 865-574-0022; E-mail – yt7@ornl.gov

Are Ballasted Roof Systems Cool?

ABSTRACT

The mass of a ballasted roof can reduce peak roof temperatures and delay the heat flow into a building. Although they perform similar functions, ballasted roofs do not meet the typical requirements set out by the Environmental Protection Agency (EPA) and other organizations for being a "cool roof." To address whether ballasted roofing systems offer energy efficiency benefits similar to those of cool roofs, a project to perform side-by-side experiments was initiated.

Three different weightings of ballasted roofs, along with three paver systems, were compared to black and white membranes. These test sections were constructed and installed on the Roof Thermal Research Apparatus (RTRA) at Oak Ridge, TN, and were monitored for thermal performance continuously for a three-year period. Data collection included continuous monitoring of temperatures, heat flows, and weather conditions, as well as periodic verification of the surface properties (solar reflectance and infrared emittance). The data was also used to validate numeric models so that the performance of ballasted systems could be extended to other climates and roofing configurations.

INTRODUCTION

Ballasted systems entered the roofing market in the early 1970s. The stone used with these systems is different from the traditional 1/4-inch chip or smaller stone used with built-up and modified bitumen roofing. With these last two systems, the small stones are partially embedded into the topcoat of asphalt to protect the asphalt (same applies to coal-tar-based systems) from the harmful ultraviolet rays of the sun. The stone used as ballast for single-ply systems is large in size, #4 (0.75 to 1.5 inch in diameter) and larger stone. Ballast comes in other forms, such as concrete or rubber pavers. Ballast is applied in loadings from approximately 10 (the minimum) to over 24 lb/ft^2. So with the loose-laid ballasted roof system, the contractor places all the components of the roof system, including the thermal barrier and insulation, unattached on the roof deck. The membrane is also loose-laid except for attachment around the perimeter of the building and at roof penetrations. The ballast is then placed on top of the membrane, weighing down all the components to hold them in place.

In recent years, new roofing membranes offering highly reflective surfaces have become the new rage of the industry, government, and code agencies. These membranes are used in fully adhered and mechanically fastened roof systems to take advantage of the reflective property of the membrane. With these systems offering aesthetically pleasing roofs that assist in saving energy for the building owner, ballasted systems now seem a little old fashioned and out of step with the times. Is this truly the case, or are there energy savings associated with the use of ballasted systems that have not been identified?

An experimental study was initiated to quantify the energy savings of ballasted roofing systems and to compare their energy performance to that of "cool roof" membranes. The experimental design was initially structured to evaluate how the mass of three different stone ballast loadings and one uncoated paver ballast affected heat flux into the building and the buildup of the membrane surface temperature in comparison to the controls. In this project, both a black and a white single-ply membrane served as controls. Two additional paver ballasts, coated with a highly reflecting white coating, were deployed a year into the project. Experimental work included the initial and subsequent occasional measure of solar reflectance and estimate of the infrared emittance of the test samples, weekly organization of the temperature and heat-flux data, and comparison of the energy performance of the systems to that of the white and black controls.

Modeling the stone for its energy performance was one of the goals of this project from the outset. The uncoated and coated paver ballasts were included to aid in developing the model. If successful, a model could eventually allow ballast to be entered as a roof component in the DOE Cool Roof Calculator (Petrie *et al.* 2001, Petrie *et al.* 2004). Such a generalization of the experimental results would permit the annual heating and cooling loads to be estimated for specific ballast configurations on roofs with various insulation levels located in different regions of the country.

This report describes the experimental work and the effort to model the energy performance of the ballasted systems for all three years of the project. The thermal and physical properties of the various configurations are used as input to the one-dimensional transient heat conduction equation that is programmed in finite difference form in Simplified

Transient Analysis of Roofs (STAR) (Wilkes, 1989). The purpose of the modeling is to achieve good agreement between two predicted and measured quantities for several clear days during the project. The properties to achieve this agreement are then used to predict cooling and heating loads for comparison to loads from the measurements.

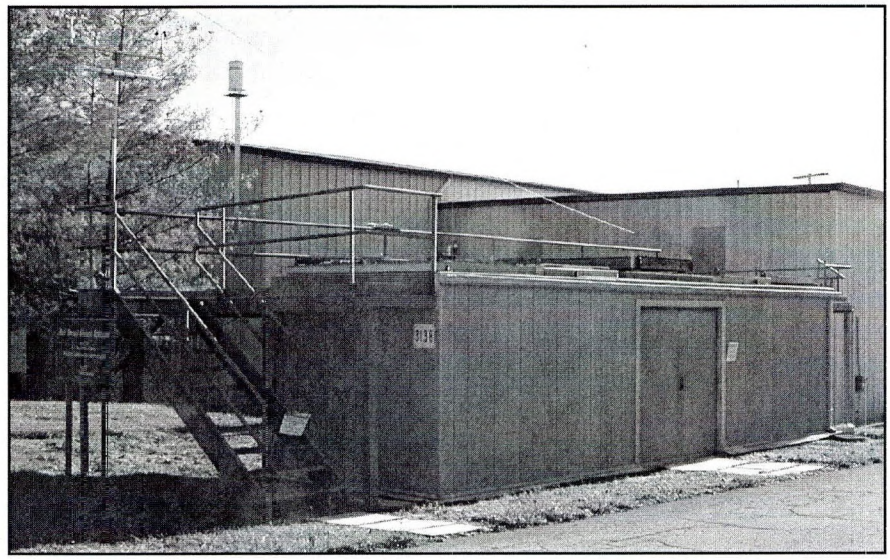

Figure 1 – Roof Thermal Research Apparatus with weather station.

Experimental Facilities

The Roof Thermal Research Apparatus (RTRA) at the Oak Ridge National Laboratory, located in Oak Ridge, TN, was constructed in the late 1980s for documenting the effects of long-term exposure of small, low-slope roof test sections to the East Tennessee climate. The RTRA has four 4-ft by 8-ft openings in its roof to receive different instrumented low-slope roof test sections. For this project, all four of the test sections are used. Each test section is divided into two 4-ft by 4-ft areas. One contains the ballast systems for the 10 lb/ft^2 and 16.8 lb/ft^2 tests. The second contains the 23.5 lb/ft^2 tests, both stone and paver. The third contains the control systems, one with a black membrane and the other with a white membrane. The fourth, deployed one year into the project, had two loadings of pavers, 21 and 16 lb/ft^2, coated with highly reflective white Decothane, a high-solids, elastomeric, single-pack polyurethane coating. *Figure 1* is a photograph of the RTRA that shows the building, including the weather station

A dedicated data acquisition system is housed inside the RTRA. It acquires the outside temperature and relative humidity and the wind speed and direction 10 ft above the roof of the RTRA. The total horizontal solar insolation and the total horizontal infrared radiation are measured at the top of the railing in *Figure 1*. There are also many dedicated input channels for thermocouples and for millivolt signals, such as those produced by heat flux transducers. Data are acquired under control of a database that is specific to each experiment. The database instructs the data acquisition program as to what data to acquire and how often. Most channels are polled every minute. Data are stored in a compressed historical record. For ongoing experiments, averages every 15 minutes of all variables are written weekly to a spreadsheet. Special reports can be generated for further detail on time dependency down to the frequency in the historical record.

Test Sections

Figure 2 is a photograph taken on top of the RTRA that shows the four test sections being used for the ballast systems project. The coated pavers and the controls are in the foreground and the ballast systems are in the background beyond an uninstrumented area for unmonitored exposure of materials. To begin construction of the ballast systems, pavers 2 in thick and 2 ft square were weighed on a scale to determine their weight per unit area. Three of the four pavers required for a 4-ft square test section were sawed in half in order not to have any seams at the center of the paver test section. A whole paver occupies the center,

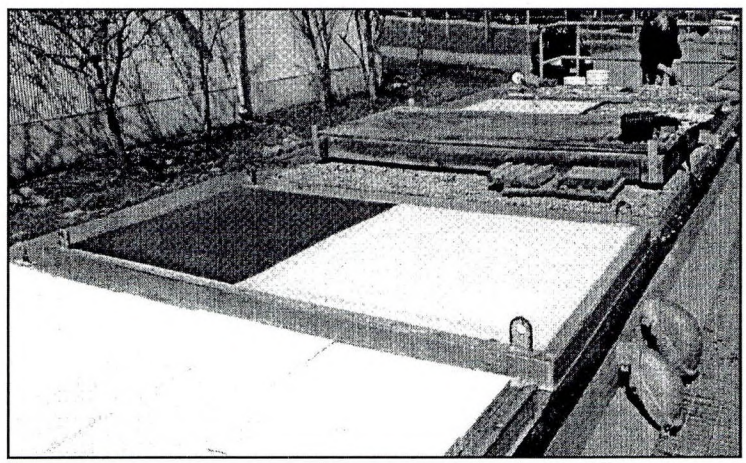

Figure 2 – Test sections configured for the ballast tests.

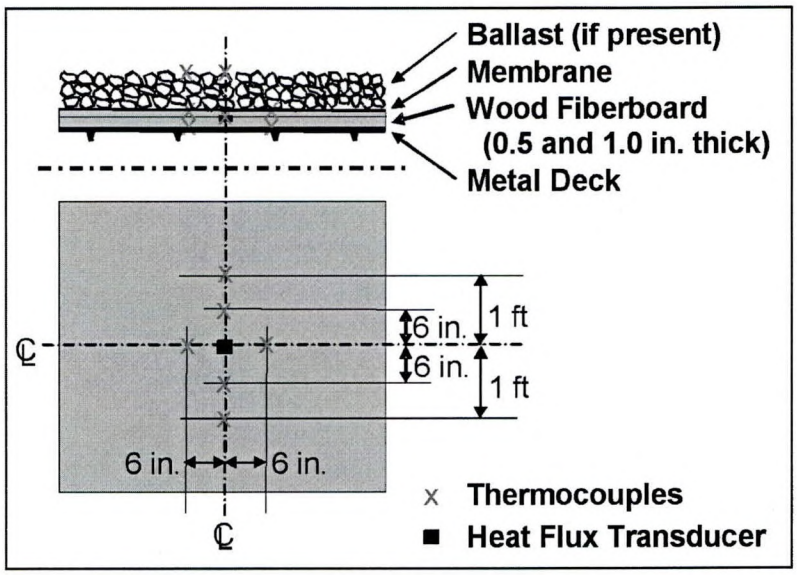

Figure 3 – Thermocouple and heat flux transducer placement relative to the center of each test section.

and halves complete it. The required weight of stone in the test area to achieve the same loading as the pavers was determined for the heaviest stone. The lightest stone ballast loading was set at 10 lb/ft^2, which is the minimum allowed for a ballast system, and it did supply 100 percent coverage of the membrane. The third ballast was set at the average of the heaviest and lightest. Buckets were used to carry the #4 stone from the scale to the roof of the RTRA, where it was distributed inside frames to confine the ballast to its assigned area. Exactly enough stone was used to achieve the 10, 16.8, and 23.5 lb/ft^2 loadings. Separate determinations were made of the weight of stone to exactly fill a bucket and the volume of the bucket. This yielded a density of 92.4 lb/ft^3 for the stone. Dividing each loading by the density of the stone yielded average thicknesses of 1.3, 2.2 and 3.1 in, respectively, for the three stone ballast systems. Due to the nature of the stone, the thicknesses vary over the area of each stone test section.

The instrumentation for each test section is shown in *Figure 3*. The metal decks are exposed to the conditions inside the RTRA, which is maintained year-round between 70 and 75°F by an electric resistance heater and a small, through-the-wall air conditioner. The membranes, in the case of the unballasted controls, or the top surfaces of the ballast, for the other test sections, are exposed to climactic conditions. Thermocouples on the decks and at the top of the test sections monitor the direct response to the imposed conditions. Additional thermocouples are at the internal interfaces. Wood fiberboard insulation 1.5 inches in thickness is used to maximize sensitivity to differences among the test sections. At the interface between 1- and 0.5 inch thick pieces of insulation, a heat flux transducer (HFT) is embedded in the top of the thicker insulation board. Each HFT was specially calibrated in the same configuration. Thermocouples are deployed at the level of each HFT, 6 and 12 inches from its center to monitor if there is any significant heat flow in the horizontal direction. Thermocouples at the other levels are 6 inches from the center of the test section.

The irregular upper surface of the stone-ballasted test sections presents a special challenge for monitoring surface temperature. *Figure 4* shows the scheme that was adopted. Aluminum wire is strung across the middle of the frame from side to side in both directions. Thermocouples are attached to the wires with plastic wire ties. The lead wire between each measuring junction and its nearest wire tie is bent to hold the

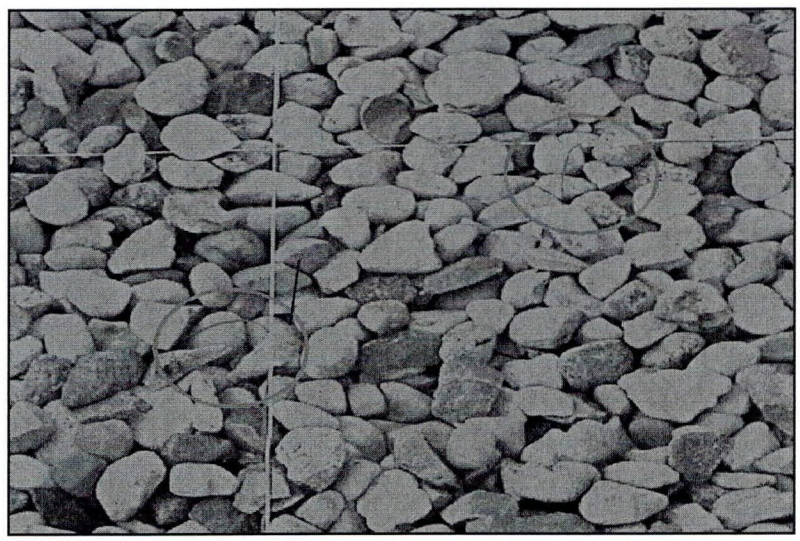

Figure 4 – Thermocouple measuring junctions placed against pieces of stone at the top of the stone-ballasted test sections.

measuring junction against a stone at the top of each test section. At the top of the paver-ballasted test section, a shallow hole was drilled into the top of the central paver, about 6 in (150 mm) from its center, and the thermocouple was epoxied in place with its measuring junction touching the bottom of the hole.

Solar reflectance, %	Summer 2004	Winter 2004	Summer 2005	Winter 2005	Summer 2006	Winter 2006
White TPO membrane	70.5	63.7	61.8	60.4	60.7	60.5
Black EPDM membrane	8.0	8.9	9.4	9.1	9.0	8.8
Uncoated paver	54.0	52.0	49.4	49.3	48.9	47.2
21 lb/ft² coated paver	--	--	72.8	71.4	70.9	71.5
16 lb/ft² coated paver	--	--	74.1	75.2	76.1	75.6

Table 1 – Variation of solar reflectance for the smooth surfaces in the project.

A property of primary interest for understanding the thermal performance of roofs is the solar reflectance of the roof surface. It was measured for the surfaces of the test sections with two different techniques. For the smooth-surfaced controls and the relatively smooth-surfaced pavers, a Devices & Services solar spectrum reflectometer was taken onto the RTRA and used according to ASTM C 1549-04, Standard Test Method for Determination of Solar Reflectance Near Ambient Temperature Using a Portable Solar Reflectometer (ASTM, 2004, and Petrie, 2000). *Table 1* summarizes the variation of solar reflectance for the smooth surfaces over the course of the project. Measurements were made near the beginning and end of each period and were interpolated to the middle of the seasons listed. The summers are six-month intervals starting in late April and ending in late October. The winters start in late October and end in late April.

The white TPO and uncoated paver showed effects of weathering. The TPO was fully weathered in less than two years. Its solar reflectance then stayed relatively constant for the rest of the project. The paver showed a similar pattern with smaller decreases, but an additional decrease in the winter of 2006. The black EPDM did not show much increase in solar reflectance, as it weathered even though graying is a common phenomenon for initially black surfaces. The coating on the pavers proved to be resistant to weathering effects during the two years of exposure. No effort was made to clean any of the surfaces in order to restore solar reflectance lost during the project due to weathering.

For the stone-covered test sections, a Davis Energy Group roof surface albedometer was taken onto the RTRA and used with guidance from ASTM E 1918-97, Standard Test Method for Measuring Solar Reflectance of Horizontal and Low-Sloped Surfaces in the Field (ASTM, 1997). From data obtained at the beginning of each year of the project, solar reflectance of the stone did not change. The average for all the stone-ballasted test sections was 20% with two standard deviations (95% confidence) about it of ±1.4%.

The albedometer measures the solar reflectance of a surface as the ratio of the output of a solar spectrum pyranometer when inverted (facing downward toward

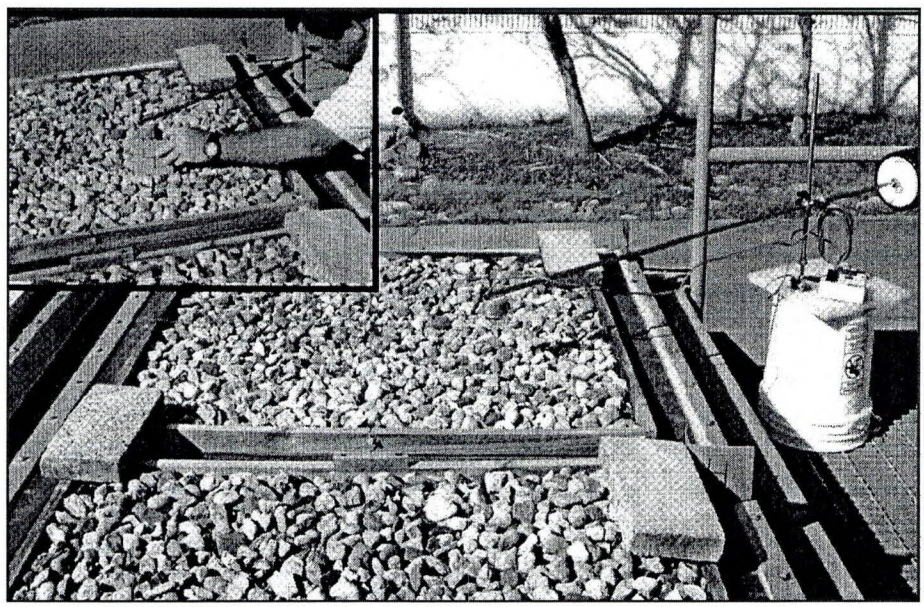

Figure 5 – Use of a custom-made albedometer to measure the solar reflectance of the 4-ft square stone-ballasted test sections. Inset shows adjustment of the height of the albedometer to 4 inches above the stone surface.

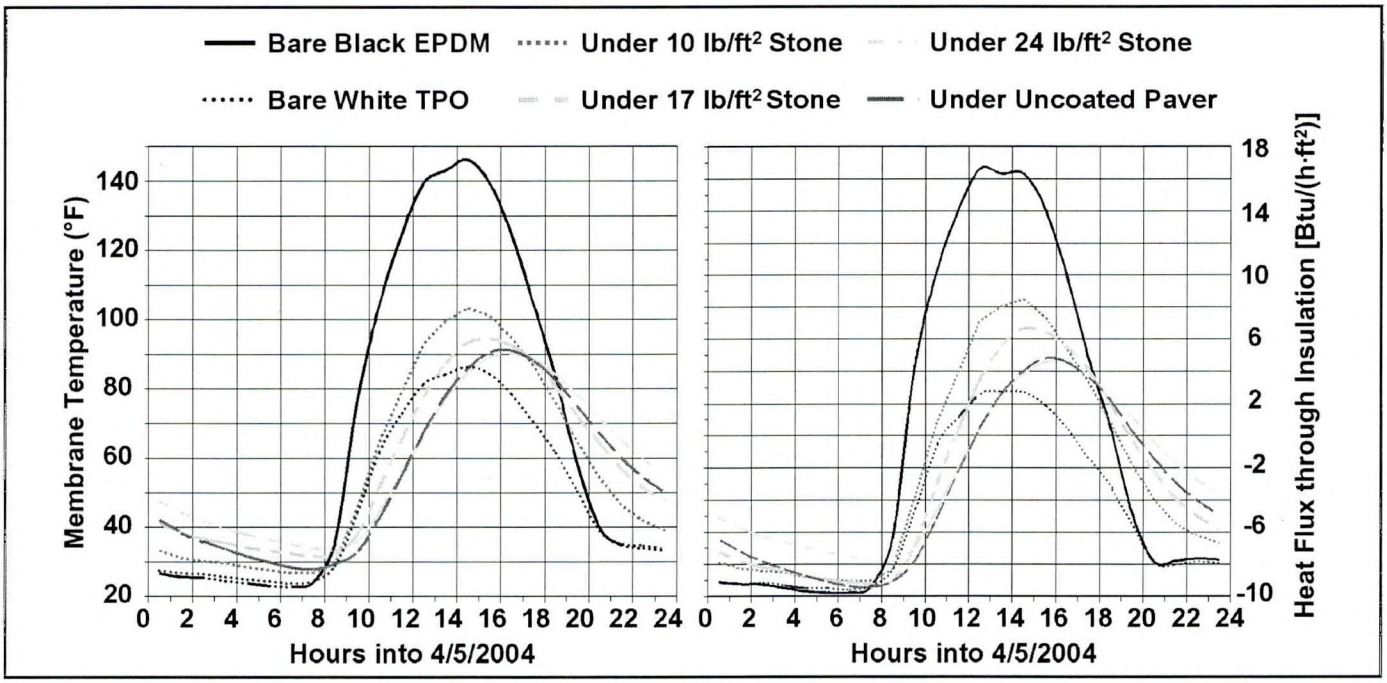

Figure 6 – Membrane temperatures and roof heat fluxes one month into experimental program.

the surface) and facing upward during an interval of constant solar irradiance. The area of the ballasted test sections is only 4 ft by 4 ft, not the 13 ft by 13 ft recommended in E 1918 for use of the instrument. In order to minimize the effect of shadows from the assembly on the test section during use of the albedometer, a standard 20-in height of the sensor above test sections is specified. It is achieved by the support stand that is part of the assembly.

Because of the relatively small size of the ballasted test sections, the standard height was relaxed to 4 in. Lack of effect of this height was verified by extensive trials. A special support stand achieved the height of 4 inches above the surfaces. The stand held the pyranometer and its support arm steady and level during the measurements. *Figure 5* is a photograph of the albedometer in place over the surface of one stone-ballasted test section.

The inset shows the designer of the custom-made albedometer, the late Ross Robertson of Firestone Building Products, adjusting it to the 4-in height. Ross brought the apparatus to Oak Ridge at the start of each year of the project to assist with the measurements. He also oversaw the fabrication and deployment of the coated pavers. His sudden and unexpected death near the end of the project meant he could not see its final results and lend his insights to conclusions from it. He was eager to contribute however he could to this project and set the standard for a contributing partner in user agreements.

A property of secondary interest for the thermal performance of roofs is the infrared emittance of the roof surface. It is difficult to measure for thermally massive systems, especially the irregular surfaces of the stone-ballasted systems. In general, non-metallic surfaces have infrared emittance near 0.9. This value is assumed to apply to all the test sections in the ballast system study and has been verified often in the SPRI study for single-ply white and black membranes.

Experimental Results

The ballast study went live on March 12, 2004 with the start of data collection, which continued uninterrupted through April 22, 2007. *Figure 6* depicts the membrane temperature and heat fluxes through the six roof assemblies for a 24-hour period on April 5, 2004. These data start at midnight (Hour 0) and were compiled approximately one month after the experiments started, but just before the Summer 2004 period in *Table 1*. Hourly averages were formed at the end of each hour and are plotted at the midpoint of the hour.

In *Figure 6*, the black membrane shows the maximum temperature, peaking at approximately 146°F. The white membrane shows the lowest peak temperature of 86°F. Between the two extremes are the temperatures for the membranes covered by the three stone ballasts and the uncoated paver. The three stone-ballasted systems have peak membrane temperatures of 103°F, 95°F, and 90°F, respectively. The

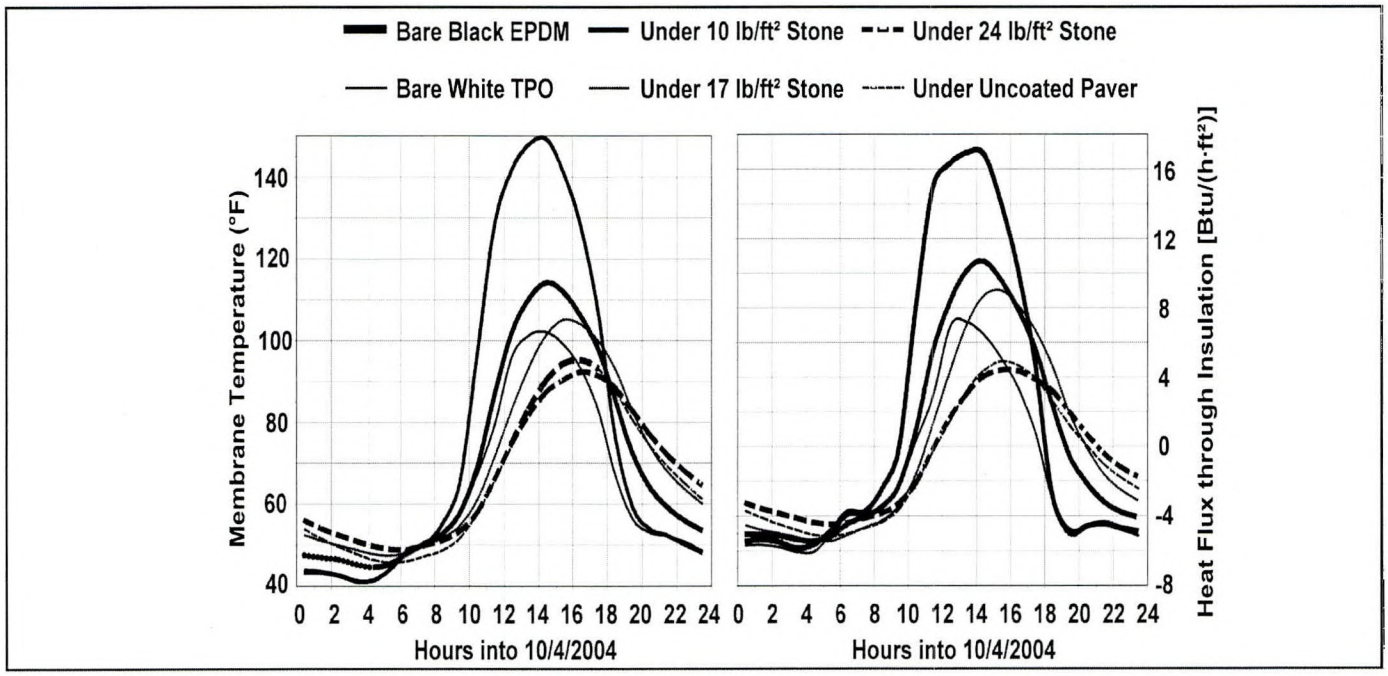

Figure 7 – Membrane temperatures and roof heat fluxes seven months into experimental program.

membrane under the uncoated paver has approximately the same peak temperature as the stone system, having the same areal density. The ballasted systems show a delay in the peak temperature that ranges from 30 minutes to two hours. The delay increases as the areal density increases. The thermal inertia of the stone and paver ballasts can also be seen in the nighttime behavior. The energy storage in the massive systems keeps them warmer throughout the nighttime hours.

The heat flux data in *Figure 6* corroborate the temperature data. Peak heat fluxes are arranged in the identical order as the peak temperatures. After one month of performance, the white membrane has the lowest peak temperature and heat flux. This suggests that it is outperforming the other roof systems in terms of reducing cooling energy loads and peak demand.

Figures 7 through 12 depict the membrane temperature and heat fluxes for the six, then eight roof assemblies for a 24-hour period on October 4, 2004; March 21, 2005; October 5, 2005; May 23, 2006; October 4, 2006; and April 22, 2007, respectively. These data start at midnight (Hour 0) and were compiled for clear days in fall and spring throughout the project. After seven months in service, as shown in *Figure 7*, the black membrane continues to have the warmest membrane, reaching a peak temperature of 150°F. Unlike in the initial results, the white membrane is no longer the coolest surface. After only seven months of service, the 24 lb/ft² stone loading, as well as the uncoated paver, now have peak membrane temperatures that are lower than that of the white system. The 17 lb/ft² ballast loading has a peak membrane temperature almost equal to that of the white membrane. Similar to what was seen in *Figure 6*, the ballast loadings delay the peak membrane temperatures and heat fluxes. Delays from one to three hours are measured and the delays increase with increasing levels of mass.

It is interesting to note that the heaviest stone-ballasted system and the uncoated paver have identical areal densities but substantially different solar reflectances. The stone and uncoated pavers have solar reflectances of 0.20 and 0.54, respectively, after seven months. Their identical performance strongly suggests that the controlling parameter is the mass and not the solar reflectance.

The heat fluxes have the same trends as the temperatures. The 24 lb/ft² stone-ballast loading, as well as the uncoated paver, now have peak heat fluxes lower than the white system, 4.5 vs. 7.0 BTU/(h·ft²). The black system has the highest peak heat flux, 17.0 BTU/(h·ft²) on the day shown.

After 12 months of exposure in East Tennessee (see *Figure 8*), the black membrane continues to be the warmest, reaching a peak temperature of 146°F. Like after seven months, the 24 lb/ft² stone-

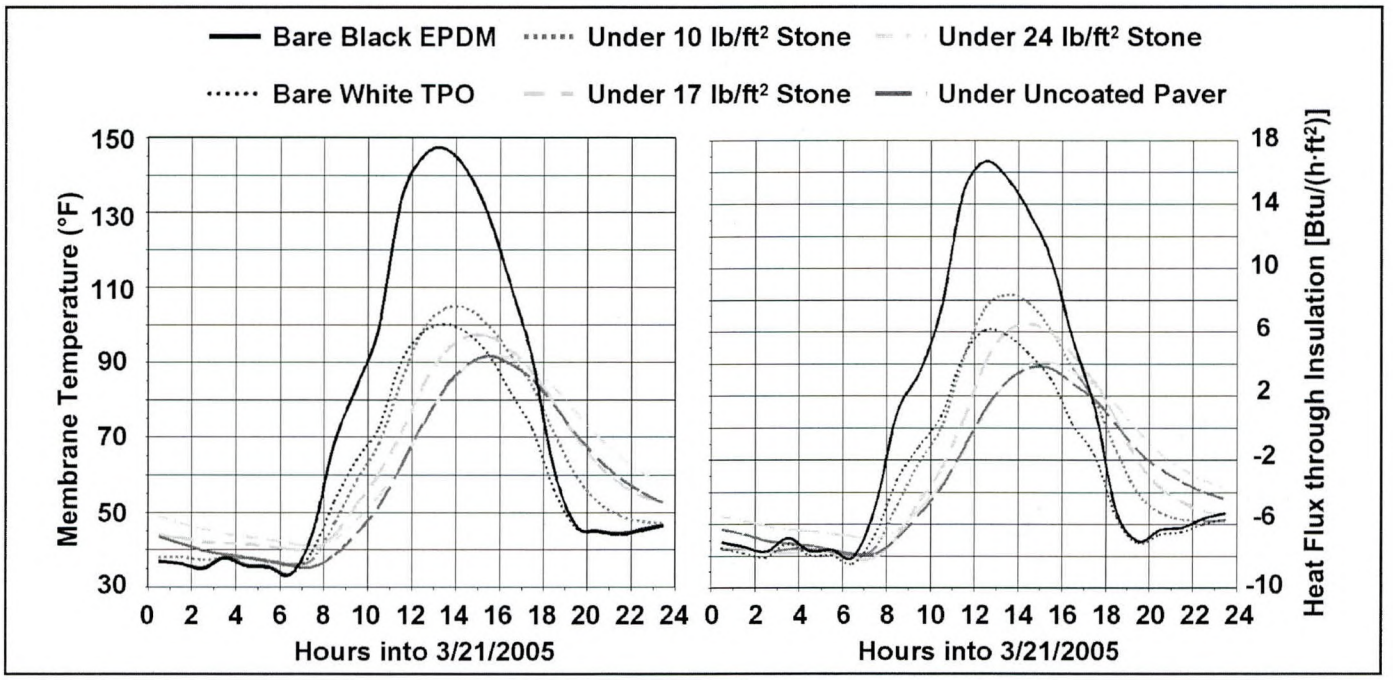

Figure 8 – Membrane temperatures and roof heat fluxes 12 months into experimental program.

ballasted system, as well as the uncoated paver, have peak membrane temperatures that are 9°F lower than the peak for the white membrane. In addition, the 17 lb/ft² ballast loading has a slightly lower peak temperature than the white membrane (approximately 1°F cooler). After twelve months, the black membrane continues to exhibit the highest peak heat flux, 16.8 BTU/(h·ft²) on this day. The 24 lb/ft² stone-ballasted system, as well as the uncoated paver, have peak heat fluxes that are 4.2 and 4.6 BTU/(h·ft²). These peaks are lower than the 7.3 and 9.0 BTU/(h·ft²) peaks for the white and 17 lb/ft² stone systems, respectively.

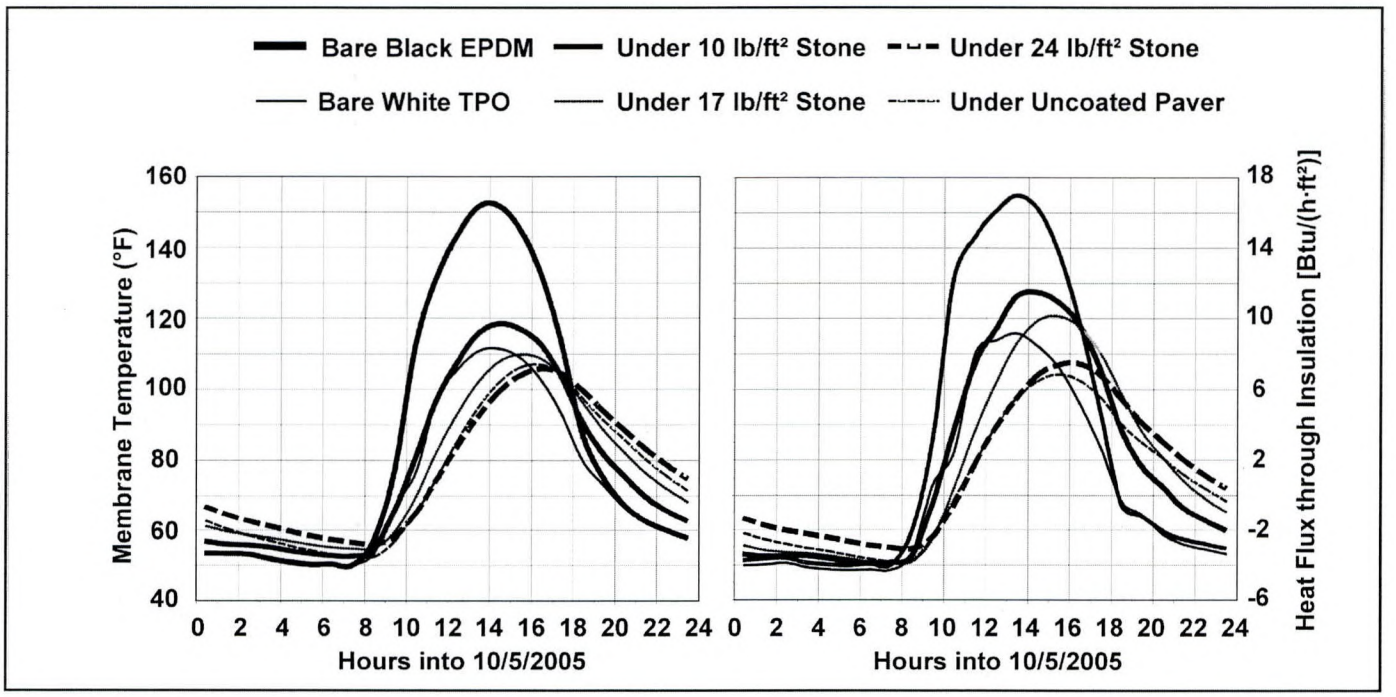

Figure 9 – Membrane temperatures and roof heat fluxes 19 months into experimental program.

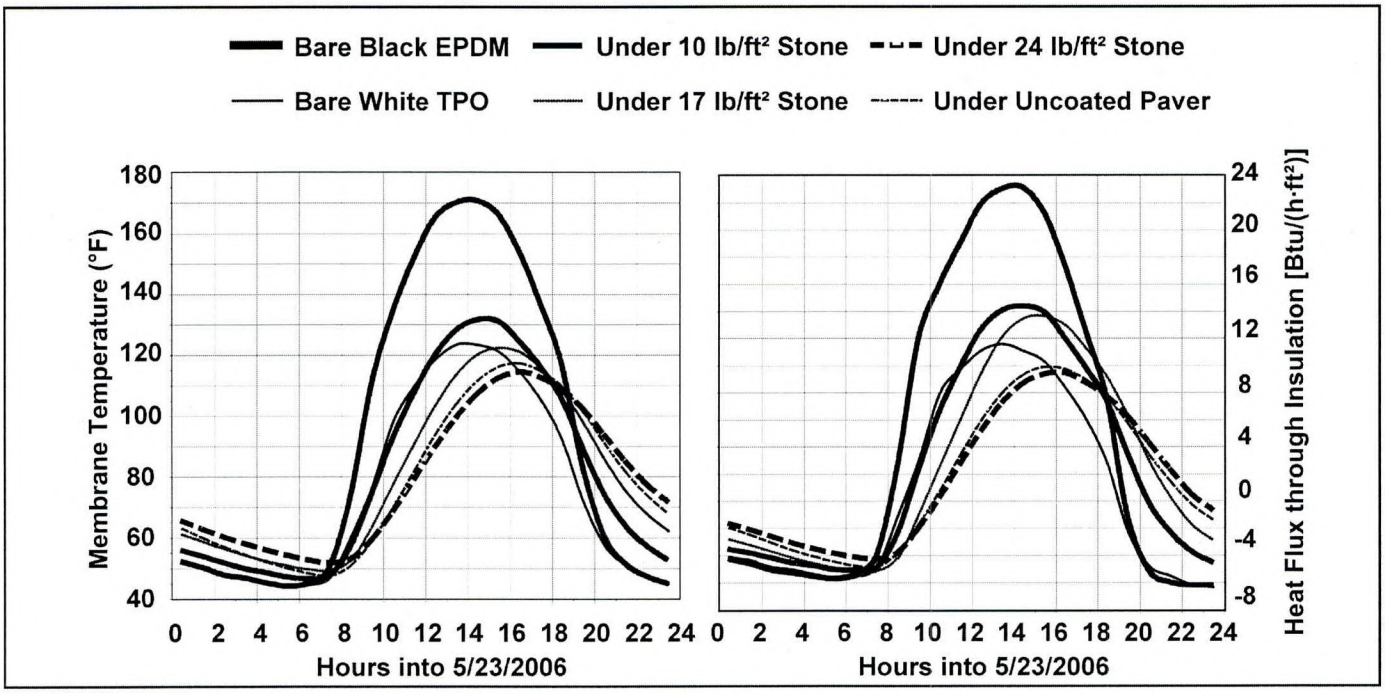

Figure 10 – Membrane temperatures and roof heat fluxes 26 months into experimental program.

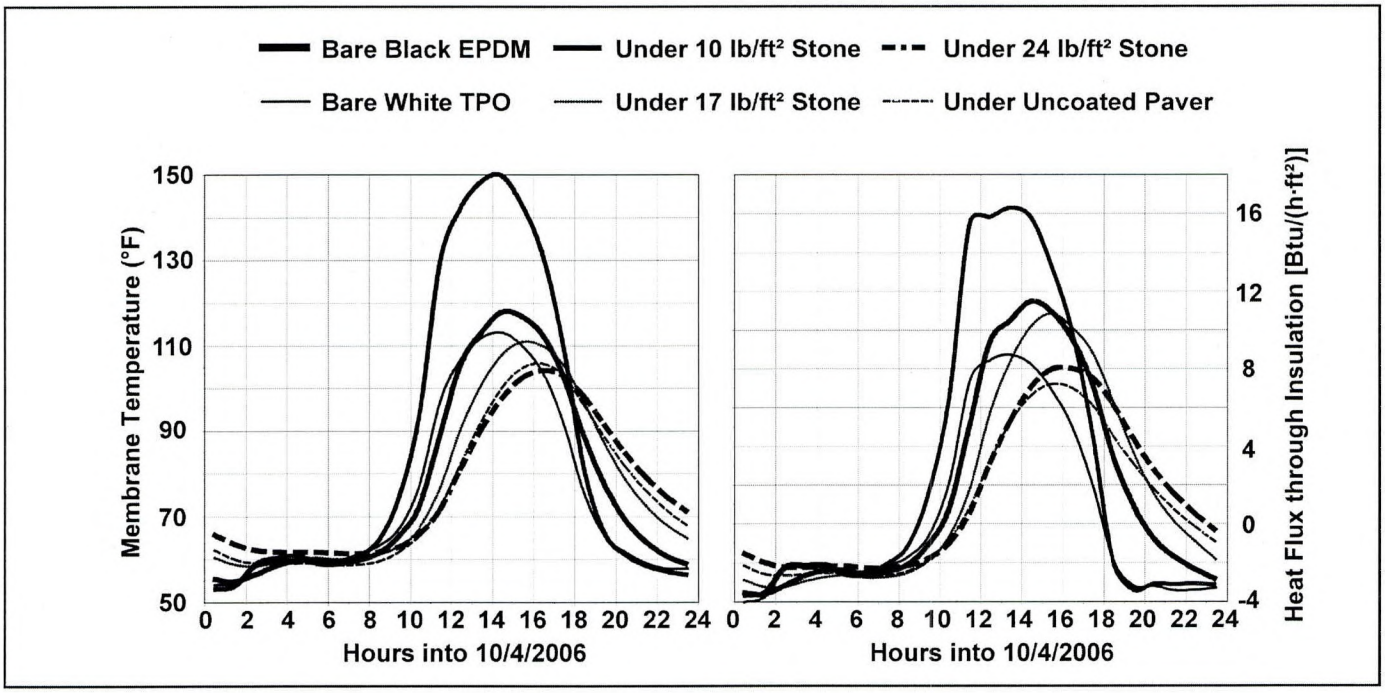

Figure 11 – Membrane temperatures and roof heat fluxes 31 months into experimental program.

After 19, 26, 31, and 37 months of exposure in East Tennessee (see *Figures 9* through *12*), all of the conclusions drawn after one year continue to be true. From a cool roof perspective, we see the heaviest stone-ballasted system and uncoated paver outperforming the white system. The medium stone-ballasted system has performance very similar to the white system. As the white membrane continues to age, its solar reflectance may continue to drop (Miller and Roodvoets, 2004), while little change is anticipated in any of the ballasted systems. Since ballasted roofing systems are expected to have a service life well in excess of ten years, their performance will continue to

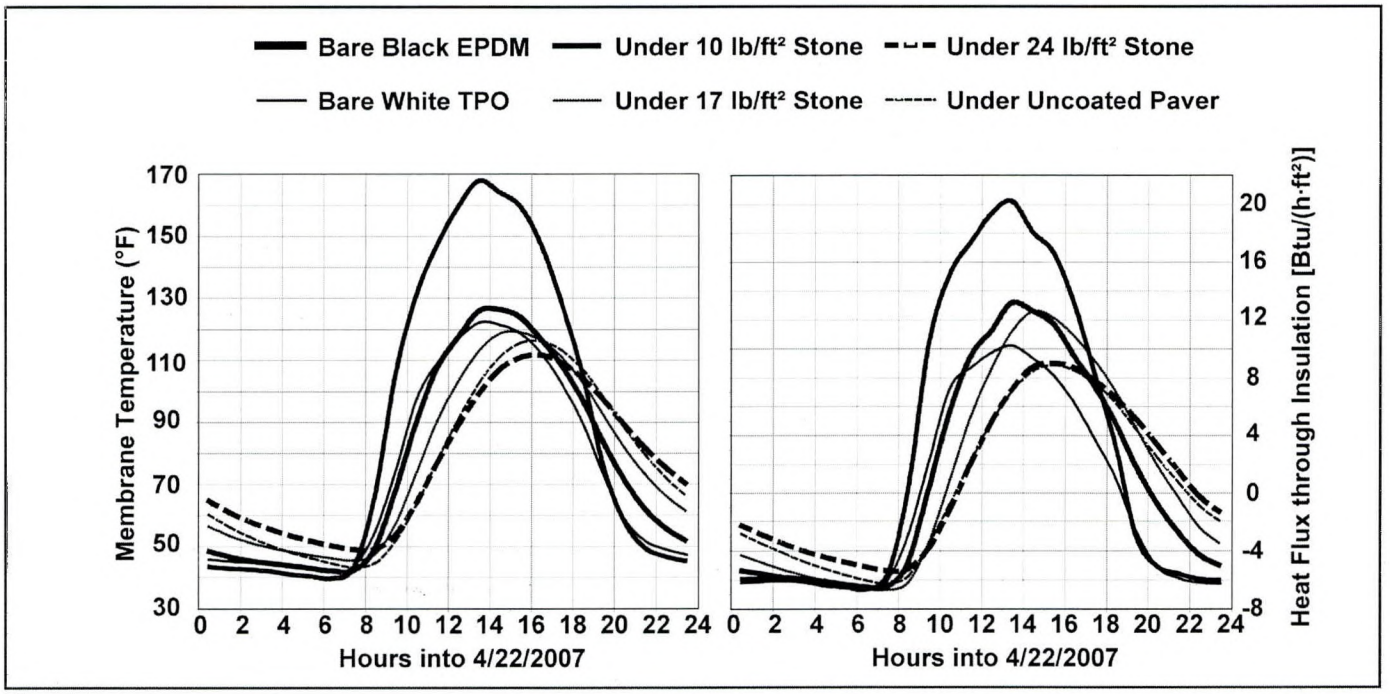

Figure 12 – Membrane temperatures and roof heat fluxes 36 months into experimental program.

exceed that of the white membrane system for over 90% of their service lives. Because the solar reflectance of the white TPO reached a relatively stable minimum after a year into this project, the relative behavior of all temperatures and heat fluxes is about the same in *Figures 9* through *12*.

Figures 9 through *12* include the membrane temperatures and roof heat fluxes for the coated pavers. The coated pavers combine the effects of high solar reflectance and high thermal mass. As expected, they perform better than any other system, showing the lowest peak membrane temperatures and heat fluxes.

Measured Heat Fluxes, Cooling Loads, and Heating Loads

The membrane temperatures presented in *Figures 6* through *12* were measured independently of the insulation heat fluxes. Therefore, they provide a useful check on the validity of the heat fluxes. After all, it is the temperature difference between the roof membrane and deck that drives heat through the roof. However, the heat fluxes are of primary interest as a measure of energy performance. Heat is what has to be removed in the form of cooling load or added in the form of heating load by the conditioning system in the building under the roof.

To analyze the heat fluxes in more detail, average yearly heat fluxes at the location of the heat flux transducer in each system (see *Figure 3*) over the course of the project were computed and summed. In the DOE Cool Roof Calculator (Petrie *et al.*, 2001; Petrie et al. 2004), cooling loads are defined as the annual sum of the positive heat fluxes through the roof deck when outside air temperature is greater than 75°F. Heating loads are defined as the sum of the negative heat fluxes through the roof deck when outside air temperature is less than 60°F. Not including the small heat fluxes between 75°F and 60°F is meant to approximate the dead band, at least that due to the roof, when the building under the roof needs neither heating nor cooling and the conditioning system is off. These definitions were applied to the heat fluxes through the insulation for the three years.

Cooling and heating loads for the white system are shown in *Table 2*. Even for this relatively simple system, changes in climatic conditions from year to year and changes in the system itself make for complicated behavior. Changes in climatic conditions are represented by the 65°F heating and cooling degree-days calculated from the outdoor temperatures measured above the test sections. Loads for the white system are affected by the changes in solar reflectance of its TPO membrane, which were shown in *Table 1*. The decrease in solar reflectance due to weathering was complete by the start of the second year. This may explain part of the increase in cooling load from the first year to the second. The increase in heating load must be weather-related. Moreover, the loads for the second and third year would have been the same

Year of Project	Cooling Load [BTU/ft²]	Cooling Degree Days [°F-day]	Heating Load [BTU/ft²]	Heating Degree - Days [°F-day]
2004	6960	1502	-22220	3614
2005	9340	1672	-23740	3947
2006	8790)	1560	-24740	4187

Table 2 – Measured cooling and heating loads for the white test section compared to heating and cooling degree-days over the three years of the project.

had climatic conditions not changed. Note that the changes in loads are at least qualitatively consistent with the changes in degree-days.

Figures 13 and 14 report the energy performance of the black and ballasted systems compared to the white system. Results are presented relative to those for the white system. This is done for two reasons. It somewhat cancels effects of changing climatic conditions from year to year. More importantly, it shows clearly the effects of the weathering of the white membrane.

For *Figure 13*, the cooling load for the white system was subtracted from the corresponding cooling load for each proposed system in each year. Positive numbers mean more cooling load than the white system. The black system behaves as expected. It has the largest cooling load relative to the white system. The difference decreases as the white membrane weathers. The thermal mass associated with the heavy stone and uncoated paver makes them perform as well for cooling as the white system in the mixed climate of East Tennessee. The light and medium loadings of stone are both better than the black system but do not have as small a cooling load as the white system. Both coated paver systems have smaller cooling loads than the white system.

For *Figure 14*, the heating load for each proposed system was subtracted from the corresponding heating load for the white system in each year. Positive numbers mean that the proposed system has more heating load than the white system. Since all systems show generally negative differences, the white system has the highest heating load, or, in other words, a heating penalty relative to the other systems. The energy advantage of the black system over the white system is significantly less heating load. This advantage decreases as the white membrane weathers. The ballasted systems show no clear trends.

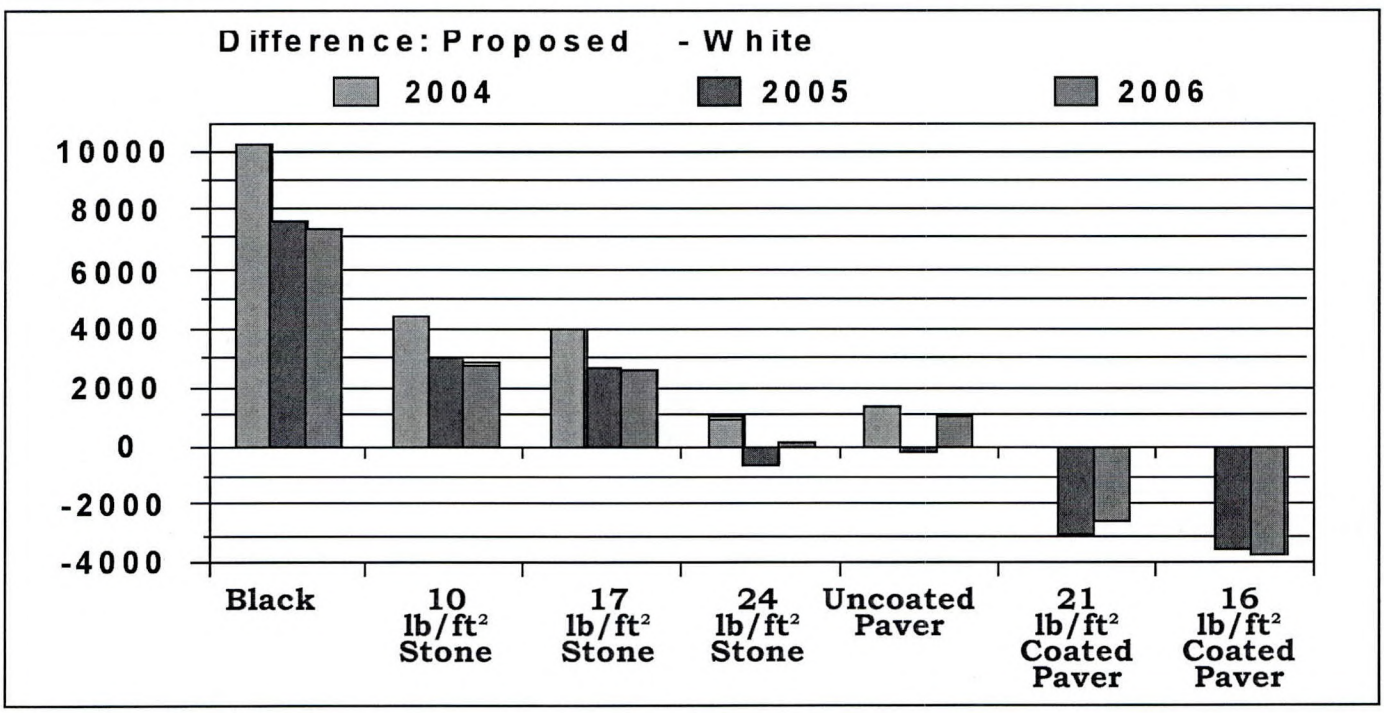

Figure 13 – Differences in cooling loads between the proposed and white systems during the years of the project.

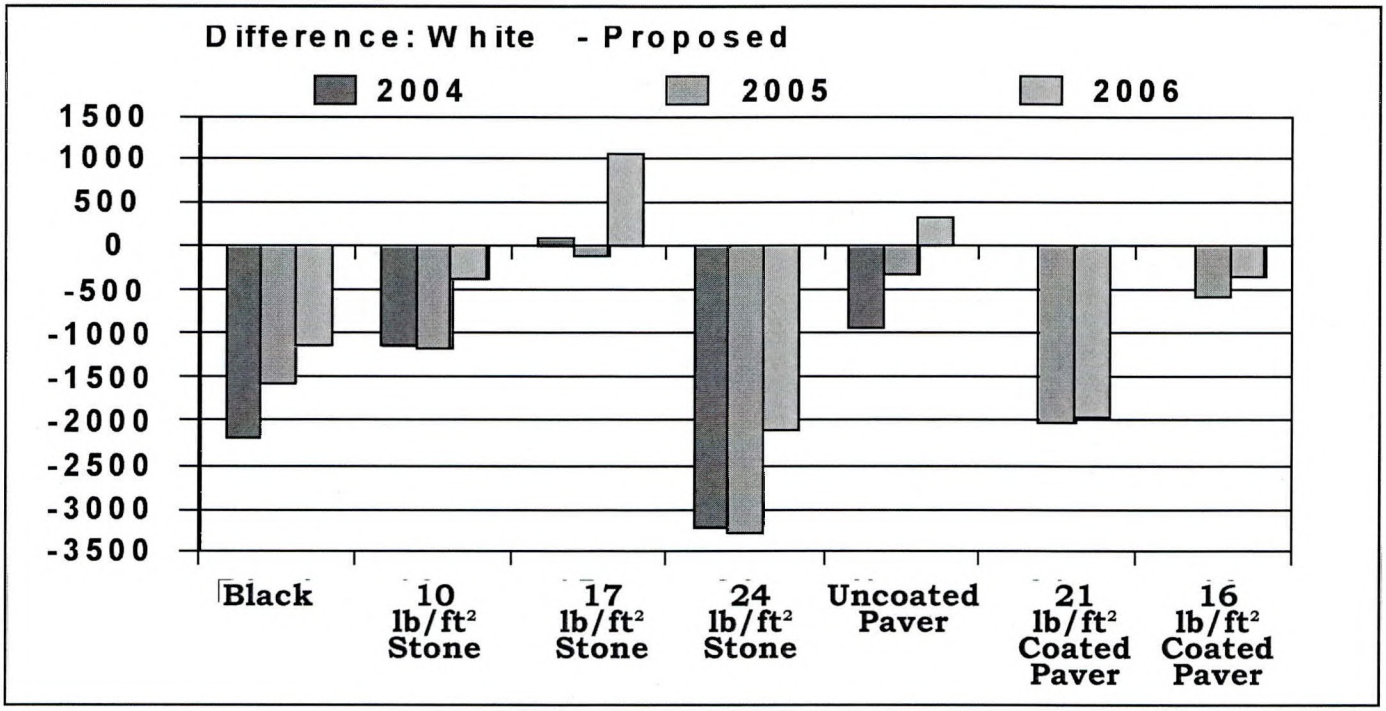

Figure 14 – Differences in heating loads between the white and proposed systems during the years of the project.

For *Figure 15*, only negative heat fluxes are used to produce the heating loads. *Figure 15* shows that there is little difference among heating loads for all these systems, including the black system, in the mixed climate of East Tennessee. As *Table 2* showed, there are enough heating degree days for the heating loads to be significant for the white system and, therefore, for

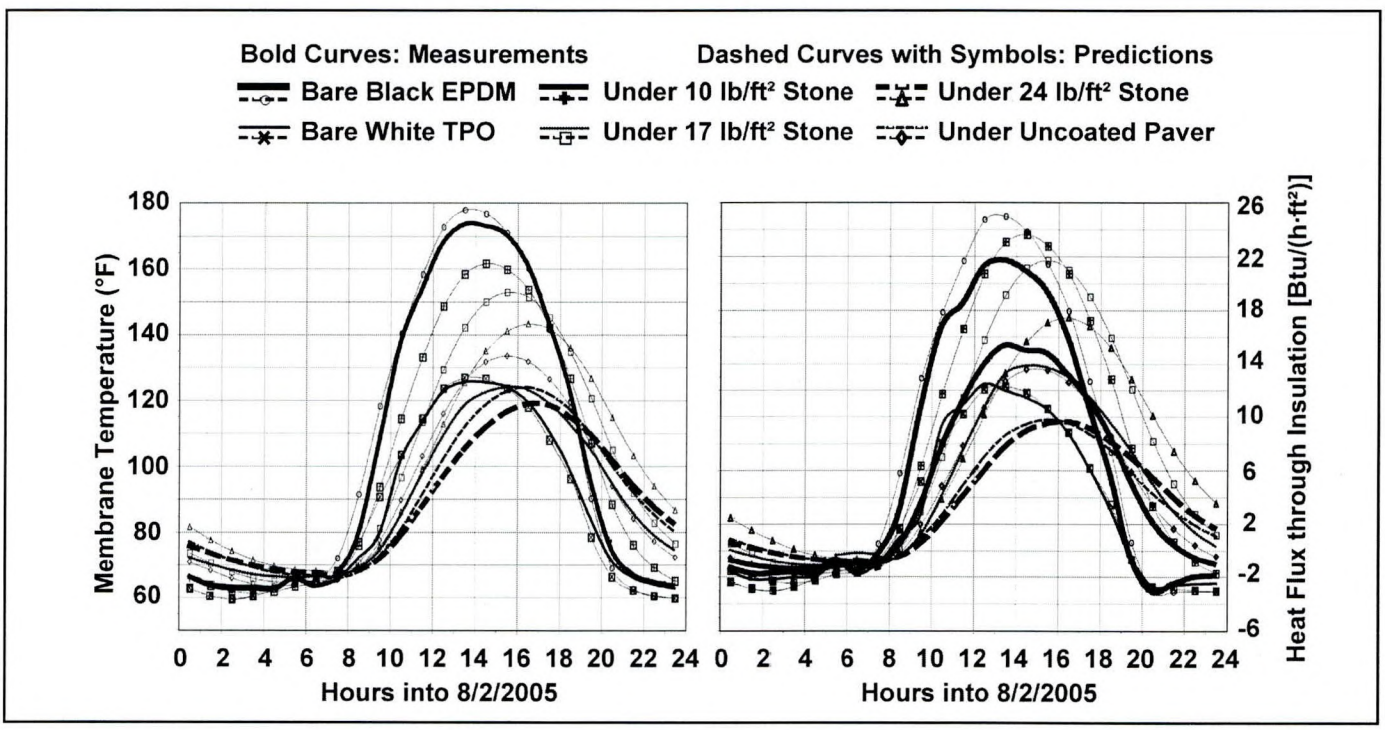

Figure 15 – Diurnal behavior of measurements and predictions using properties in Tables 1 and 3 for a typical clear day during summer 2005.

all systems.

The 24 lb/ft² stone-ballasted system and possibly the 21 lb/ft² coated paver show smaller heating loads than the black system. This may be due to the effect of thermal mass. In the case of the 24 lb/ft² stone-ballasted system, however, smaller heating loads than the black system are likely due to effects of rain. This system was positioned on the higher end of the roof, but any rain that accumulated in it had a difficult time draining because the uncoated pavers blocked it. In the weekly summaries generated to compare evolving data, it was noticed that the 24 lb/ft² stone-ballasted system took several more days than the other systems to recover from rain events. During these times, it performed more like the systems with coated pavers than the system with uncoated pavers.

Figures 14 and *15* apply only to the low R-value roofs for the climatic conditions in East Tennessee during the three years of the project. They provide experimental evidence that neither the cooling loads nor the heating loads are much different for conventional, uncoated ballasted systems and the white system. This supports the conclusion of Desjarlais *et al.* (2006) after two years that ballasted systems should be considered for "cool" status and the savings this implies. Possible operating cost savings depend not only on the heating and cooling loads, but also on the efficiency of the heating, ventilating, and cooling equipment and the price of energy to run it. Equipment efficiency and energy prices should be the same for dealing with different roofs if they cause the same loads.

Modeling the Energy Performance with STAR

To fulfill the goals of the project, an effort was made to model the behavior of the ballasted and control systems. Because of its use for the DOE Cool Roof Calculator and our extensive experience with it, the program STAR was chosen. It is a finite-difference form of the transient heat conduction equation in one dimension. All three types of boundary conditions are allowed at the inside and outside surfaces of a low-slope roof system. In the validation of the modeling for this project, the temperature measured at the top of the deck was used as the inside boundary condition. Data from the weather station on the test facility were used to impose convection and thermal radiation as the boundary condition at the outside of each system.

STAR requires a layer-by layer-description of the physical and thermal properties of roof systems. The physical layout of the systems was shown in *Figure 3*. *Table 3* lists properties for initial runs of STAR. Data are listed for the three loadings of stone, the uncoated paver, the coated pavers, the exposed white and black membranes, and the two layers of wood fiberboard insulation that were used in each system.

Direct measurements were made of the thickness and density of the various components of the systems. The weight of several pavers of each type was measured by a scale and divided by the measured volume-to-yield density. A nominal 5-gallon bucket was weighed, filled with stone, and weighed again. The actual volume of the bucket was determined by measuring the weight of water to fill it. Weight-of-stone divided by its volume yielded the average density of the stone, including air spaces. The weight of water to fill the spaces around the stones yielded a porosity of 40%. *Table 2* includes the ranges of solar reflectance for all surfaces that weathered, spanning the data presented in *Table 1* for the smooth surfaces. Solar reflectance for the stone and the estimated infrared emittance for all surfaces are repeated from the discussion above of the test sections.

The thermal conductivity and specific heat of the white and black membranes and fiberboard were obtained from the literature and our own measurements. For the stone and pavers, the program Properties Oak Ridge (PROPOR) was used as part of the ongoing analysis of evolving data to estimate effective thermal conductivity and volumetric heat capacity (the product of density and specific heat). PROPOR compares temperatures and heat fluxes that are measured inside a system to those predicted by the transient heat conduction equation. Temperatures measured at the outside and inside surfaces are boundary conditions. Thermal conductivity and volumetric heat capacity are considered parameters. Values of the parameters are adjusted by an automated iteration procedure until best agreement is obtained. Best agreement is defined as the minimum of the squares of the differences between measured and predicted temperatures and heat fluxes inside the systems. An estimate of the confidence in the final parameter values is included as part of the output from the program (Beck *et al.*, 1991).

Use of PROPOR, which like STAR is based on a finite-difference form of the transient heat conduction equation, indicated that modeling the energy performance for the ballasted systems would be more difficult than for the black and white systems. PROPOR had difficulty converging to estimates of the thermal conductivity and volumetric heat capacity for the 10 lb/ft² and 17 lb/ft² loadings of stone, except for several weeks during each winter in East Tennessee. Even then, the estimates were not acceptably precise. Convergence for the 24

Component	Loading, lb/ft²	Thickness (inches)	Thermal conductivity, BTU·in/(h·ft²·°F)	Density lb/ft³	Specific heat, BTU(lb·°F)	Infrared emittance, %	*Solar reflectance, %
10 lb/ft² stone	10.0	1.3	6.21±6	92.4	0.17±0.2	90	20
17 lb/ft² stone	16.9	2.2	5.94±7	92.4	0.21±0.3	90	20
24 lb/ft² stone	23.9	3.1	4.65±2	92.4	0.20±0.1	90	20
Uncoated paver	23.5	2.0	17.6±4	141	0.15±0.04	90	54 to 47
21 lb/ft² coated paver	21.4	1.69	6.13± 1	152	0.11± 0.03	90	73 to 71
16 lb/ft² coated paver	16.5	1.25	3.65± 0.7	158	0.083± 0.03	90	74 to 76
White membrane	negl.	0.050	1.2	58	0.4	90	70 to 60
Black membrane	negl.	0.045	1.2	58	0.4	90	8 to 9
Fiberboard	n.a.	0.5, 1.0	**a+b·T	17.5	0.19	not needed	not needed

* Ranges, if given, span observed variation over the three years of the project (see Table 1)
** From guarded hot plate measurements: $k_{fiberboard}$ [BTU·in/(h·ft²·°F)] = 0.3376 + 0.000746·T(°F)

Table 3 – Properties input to STAR for initial modeling of the ballasted and control systems.

lb/ft² stone was less difficult. Convergence was obtained for the pavers no matter what the weather conditions.

One reason for the problems with convergence and lack of confidence is convection effects in loadings of stone during peak solar insolation. Another reason is inaccurate measurement of outside surface temperatures for all the ballasts. Unlike STAR, PROPOR requires temperatures at the surface as the only allowed type of boundary condition. For the ballasts, thermocouple measuring junctions were placed against two stones at the top of each stone loading (see *Figure 4*) and slightly below the outside surface of the central paver for the uncoated and coated paver systems. Unreliable surface temperatures are more likely for the loadings of stone when the sun is high in the sky. Sunlight can penetrate as far as the black membrane and cause heating of the stones from below in addition to the usual heating from above.

The thermal conductivity and specific heat for the stone and paver systems in *Table 3* are the averages of estimates from PROPOR for weeks when it converged. The uncertainty reported by PROPOR is appended to these estimates. Specific heat is obtained by dividing the estimated volumetric heat capacity by the measured density. Only the volumetric heat capacity is used by PROPOR and STAR. The uncertainties in the estimates for both properties of the stone are of the order of 50% to 150% of the estimates themselves. Furthermore, effective thermal conductivity and, to a lesser extent, specific heat, vary with stone loading. This would not be true if heat transfer through the stone were strictly a heat conduction phenomenon, or at least apparent thermal conduction, like conduction and radiation in mass insulation. The three loadings were obtained with the same stone; only the thickness was changed.

The 0.19 to 0.24 BTU/(lb·°F) range for specific heat of heavyweight concrete (ASHRAE 2005) and the specific heat of 0.24 BTU/(lb·°F) for air compare well to values for the ballast in *Table 3*. ASHRAE handbook values of the thermal conductivity of heavyweight concrete are given as the range from 9.0 to 18.0 BTU·in/(h·ft²·°F), which includes the values for the uncoated paver but not the coated pavers in *Table 3*. Possible values for the thermal conductivity of the stone are given by Côté and Konrad (2005). The porosity of the stone was measured as 40%. Côté and Konrad's data for granite and limestone show a thermal conductivity of 1.80 BTU·in/(h·ft²·°F) at this porosity, 29 to 39% of the values for the stone ballasts in *Table 3*.

An attempt was made to measure the thermal conductivity at 75°F of the stone and pavers by ASTM C518-98: Standard Test Method for Steady-State Heat Flux Measurements and Thermal Transmission Properties by

Means of the Heat Flow Meter Apparatus (ASTM, 1998). Samples of the stone and uncoated paver were sandwiched between pieces of foam to protect the apparatus and provide the required level of thermal resistance. The foam used was characterized separately. Differences between R-values and thicknesses with and without the stone yielded stone sample thermal conductivity of 1.86 BTU·in/(h·ft²·°F) for heat flow up and 1.76 BTU·in/(h·ft²·°F) for heat flow down. The average 1.81 BTU·in/(h·ft²·°F) agrees with the data from Côté and Konrad. Slightly higher thermal conductivity for heat flow up is consistent with the effect of air between the individual stones. By the same technique, the uncoated paver had thermal conductivity of 6.58 BTU·in/(h·ft²·°F), 27% of the value in *Table 3*.

STAR was executed with the properties in *Tables 1* and *3*, yielding hourly predictions of membrane temperatures and insulation heat fluxes for all three years of the project. Because of the large uncertainty of their estimation by PROPOR and the low values of thermal conductivity indicated by the literature and the C 518 measurements, it was unlikely that they would yield acceptable agreement with measurements.

The predicted membrane temperatures and insulation heat fluxes were entered in a spreadsheet that contained the hourly averages of the measurements. Graphs were generated for selected days to show diurnal behavior and indicate agreement between measurements and predictions. Clear days show maximum solar effect and have smooth curves through the hourly temperatures and heat fluxes. There are few deviations caused by cloudiness and inclement weather that make it difficult to visually compare the data. *Figure 15* shows a typical clear day during the second summer of the project, by which time the solar reflectance of the white surface had decreased to 62%.

The black and white systems are lightweight systems with R-3.8 fiberboard insulation. The ballasted systems are thermally massive with the same insulation. Thicknesses from *Table 3* and our measurements of apparent thermal conductivity with ASTM C 518 yield additional R-value of 0.7, 1.2 and 1.7 for the 10 lb/ft², 17 lb/ft² and 24 lb/ft² stone-ballasts, respectively. The uncoated paver, 21 lb/ft² coated paver, and 16 lb/ft² coated paver add R-value of 0.3, 0.3, and 0.2, respectively. *Figure 15* shows that peak values of the measured membrane temperature and insulation heat flux and the times when peaks occur are affected by the thermal mass and, possibly, extra R-value of the ballasts.

The time at which peak heat flux occurs is important to operation of the building under a low-slope roof system. Measurements for the ballasted systems show consistent delays relative to the black and white systems. For eight clear days over the course of the project, comprising the days selected for *Figures 6* through *12* and, later, *Figure 15*, the average times of peak heat flux for the white and black systems coincide within 0.2 h. Relative to the black system, the 10 lb/ft², 17 lb/ft², and 24 lb/ft² stone-ballasts show delays of 1.0 h, 1.8 h, and 2.7 h, respectively. The uncoated paver, 21 lb/ft² coated paver, and 16 lb/ft² coated paver show delays of 2.3 h, 2.6 h, and 1.8 h, respectively. This variation generally agrees with the variation of the loading of the respective systems in *Table 3*. The delays are clearly not consistent with added R-value because the pavers show delays like the medium and heavy stone loadings. This proves that the ballasted systems show significant and consistent effect of their thermal mass.

The relatively simple behavior of exposed white and black membranes over a low-slope roof with low thermal mass is well understood from previous experience with test sections used to validate STAR for the DOE Cool Roof Calculator (Petrie, 2001). On the clear days, the hourly predictions for the exposed white membrane were in good agreement with the measurements and consistent with our understanding. The hourly behavior of the exposed black membrane, when compared to that from previous experience, indicates that the measured temperatures are accurate but the measured heat fluxes are low. Temperatures and heat fluxes were measured independently with thermocouples and small heat flux transducers, respectively. More uncertainty in measured heat fluxes is consistent with our experience. It occurs despite calibration of the heat flux transducers in the wood fiberboard insulation according to ASTM C 518.

The shape of the predicted curves on the clear days is correct for the control systems, with low thermal mass and either an exposed white or black membrane. Predicted peak times coincide with the measured peak times. The nighttime predictions are generally low for both these controls. This is likely due to the effects of condensation and no attempt was made to model its effect.

Little positive can be said about the predictions of membrane temperature and insulation heat flux for the ballasted systems with properties in *Table 3*. Peak times generally coincide with measured peak times. Agreement in early morning between predictions and measurements is acceptable for the light and medium loadings of stone, but not for

the heavy stone loading or any of the pavers. However, predicted peak values for all ballasted systems are significantly higher than the corresponding peak measurements. This is the dominant feature of *Figure 15* and precludes having any confidence in the accuracy of the predictions, night or day, using the set of properties in *Table 3*.

CONCLUSIONS

Three full years of continuous monitoring in the mixed climate of East Tennessee yielded data to compare the energy performance of six ballasted systems and a system with an exposed black membrane to that of a system with an exposed white membrane. Heat fluxes through the insulation in each test section were used to obtain the annual cooling and heating loads due to unit area of each system. The cooling loads for the heavy stone-ballasted and uncoated paver-ballasted systems were approximately the same as for the white system. Cooling loads for the light and medium-weight stone systems were slightly larger than for the white system but significantly less than for the black system. Cooling loads for coated pavers with heavy and medium loading showed cooling loads significantly less than for the white system. Only the cooling load of the white system showed significant effects of weathering, which was complete by the start of the second year of the project.

Heating loads for the ballasted systems showed random variation as loading increased and type changed. Except for the heavy-weight stone system, they were about the same as for the white system. The heavyweight stone system showed slightly less heating load than the black system, but this is considered an anomaly due to rain effects. All evidence on clear days of diurnal behavior showed the heavyweight stone and uncoated paver systems performing equally, due to the same thermal mass, despite different solar reflectance.

An effort was made to model heat flow through the ballasted systems with transient heat conduction alone, using the program STAR. STAR has successfully modeled non-ballasted systems in past projects and did so again in this project. Using our best guess of properties, we were unsuccessful in this task. Further work that is now underway will look more completely at this issue. A trial-by-error analysis is planned to develop insight into this problem. It is concluded that transient heat conduction alone is not adequate to predict energy loads for ballasts.

REFERENCES

ASHRAE. 2005. *2005 ASHRAE Handbook: Fundamentals*,"Chapter 25, Table 4; Chapter 39, Table 3. Atlanta: American Society of Heating, Refrigerating and Air Conditioning Engineers, Inc.

ASTM, 1997. ASTM E 1918-97, Standard Test Method for "Measuring Solar Reflectance of Horizontal and Low-Sloped Surfaces in the Field." ASTM International, Philadelphia PA.

ASTM, 1998. ASTM C 518-98, Standard Test Method for "Steady-State Heat Flux Measurements and Thermal Transmission Properties by Means of the Heat Flow Meter Apparatus." ASTM International, Philadelphia PA.

ASTM, 2004. ASTM C 1549-04, Standard Test Method for Determination of Solar Reflectance Near Ambient Temperature Using a Portable Solar Reflectometer." ASTM International, Philadelphia PA.

Beck, J.V., Petrie, T.W. and Courville, G.E., 1991. "Using Parameter Estimation to Analyze Building Envelope Thermal Performance," pp. 161-191, Special Report 91-3. *In-Situ Heat Flux Measurements in Buildings: Applications and Interpretations of Results*. S.N. Flanders, Editor. Hanover, NH: U.S. Army Cold Regions Research and Engineering Laboratory.

Côté, J. and Konrad, J-M., 2005. "Thermal Conductivity for Base-Course Materials," pp. 61-78, *Canadian Geotechnical Journal*, Vol. 42, No. 11.

Desjarlais, A., Petrie, T., Miller, W., Gillenwater, R., and Roodvoets, D., 2006 "Evaluating the Energy Performance of Ballasted Roof Systems," presented at and published in the *Proceedings of 3rd International Building Physics Conference*, Montreal, August 27-31, 2006.

Petrie, T.W., Desjarlais, A.O., Robertson, R.H., and Parker, D.S., 2000. Comparison of Techniques for In-Situ, Non-Damaging Measurement of Solar Reflectance of Low-slope Roof Membranes, 14th Symposium on Thermophysical Properties, *International Journal of Thermophysics*, Boulder, CO: National Institute of Standards and Technology.

Petrie, T.W., Atchley, J.A., Childs, P.W. and Desjarlais, A.O., 2001. "Effect of Solar Radiation Control on Energy Costs - A Radiation Control Fact Sheet for Low-Slope Roofs," in *Proceedings of Performance of the Ex-*

terior Envelopes of Whole Buildings VIII: Integration of Building Envelopes. Atlanta: American Society of Heating, Refrigerating and Air-Conditioning Engineers, Inc.

Petrie, T.W., Wilkes, K.E. and Desjarlais, A.O., 2004. "Effect of Solar Radiation Control on Electricity Demand Costs - an Addition to the DOE Cool Roof Calculator," in *Proceedings of Performance of Exterior Envelopes of Whole Buildings IX*. Atlanta: American Society of Heating, Refrigerating and Air Conditioning Engineers, Inc.

Wilkes, K.E., 1989. Model for Roof Thermal Performance. ORNL/CON-274. Oak Ridge, TN, Oak Ridge National Laboratory.